

Intermediate-energy Coulomb excitation of  $^{19}\text{Ne}$ G. Hackman,<sup>1,2</sup> Sam M. Austin,<sup>2,3</sup> T. Glasmacher,<sup>2,3</sup> T. Aumann,<sup>2,\*</sup> B. A. Brown,<sup>2,3</sup> R. W. Ibbotson,<sup>2,†</sup> K. Miller,<sup>2,3</sup> B. Pritychenko,<sup>2,3</sup> L. A. Riley,<sup>4</sup> B. Roeder,<sup>2</sup> and E. Spears<sup>2,3</sup><sup>1</sup>*Department of Physics and Astronomy, University of Kansas, Lawrence, Kansas 66045*<sup>2</sup>*National Superconducting Cyclotron Laboratory, Michigan State University, East Lansing, Michigan 48824*<sup>3</sup>*Department of Physics and Astronomy, Michigan State University, East Lansing, Michigan 48824*<sup>4</sup>*Department of Physics and Astronomy, Earlham College, Richmond, Indiana 47374*

(Received 12 January 2000; published 5 April 2000)

Transition rates from the ground to selected states in  $^{19}\text{Ne}$  have been measured by their gamma yield following intermediate-energy radioactive ion beam Coulomb excitation. These are compared to corresponding transitions in  $^{19}\text{F}$  and to shell model calculations. An upper limit on the cross section of the 4.033 MeV state places a limit on the transition rate and hence on total electromagnetic decay width  $\Gamma_\gamma$  of this state, which is of astrophysical interest. Combining the results with an upper limit on the lifetime of this state and shell model calculations gives an estimate of its width.

PACS number(s): 26.50.+x, 21.10.Ky, 25.70.De, 27.20.+n

Electromagnetic transition rates in  $^{19}\text{Ne}$  are of both theoretical and astrophysical interest (see Fig. 1). A comparison with  $^{19}\text{F}$  provides a test of isospin symmetry in a situation where detailed *s-d* shell calculations are tractable [1]. Furthermore, the transition rates can be directly related to level widths that help determine the astrophysical reaction rate of the  $^{15}\text{O}(\alpha, \gamma)^{19}\text{Ne}$  reaction. This rate determines the conditions of temperature and density for break out of the hot CNO cycle in explosive burning scenarios such as those that occur in nova explosions or in x-ray bursts. Such a break out leads to a flow process through proton rich nuclei and results in an increased rate of energy production [2].

The 4.033 MeV  $3/2^+$  state dominates this rate owing to its proximity to energy threshold and the fact that it can be reached from the  $^{15}\text{O}$   $1/2^-$  ground state by an angular momentum of  $l=1$ . The gamma width  $\Gamma_\gamma$  for the 4.033 MeV state is much larger than the alpha width  $\Gamma_\alpha$  [3–5]. In this circumstance the reaction rate depends only on the excitation energy of the state, which is well known, and on  $\Gamma_\alpha$ , which is poorly known. Given the value of  $\Gamma_\gamma$ , one could obtain  $\Gamma_\alpha$  from a measurement of the branching ratio  $\Gamma_\alpha/\Gamma_\gamma$ . Neither of these quantities is known at present, and estimates of the rate are based on the value of  $\Gamma_\alpha$  for the analog of the 4.033 MeV state, located at 3.908 MeV in  $^{19}\text{F}$  [5]. It has been argued that such estimates are uncertain by as much as an order of magnitude [6].

We have determined reduced transition probabilities involving four excited states in  $^{19}\text{Ne}$  from their  $\gamma$  yields following intermediate-energy Coulomb excitation of radioactive  $^{19}\text{Ne}$ . The results are compared to corresponding states in the mirror nucleus  $^{19}\text{F}$  and to modern *p-s-d* shell model calculations. The measurements yield an upper limit on the reduced transition probability for the 4.033 MeV  $3/2^+$  state,

and combining this result with an upper limit on the lifetime of the state and with the shell-model calculation yields a gamma width of  $12_{-5}^{+9}$  meV.

The experiment was typical of radioactive-beam Coulomb excitation experiments at the National Superconducting Cyclotron Laboratory (NSCL) [7]. A primary beam of  $^{20}\text{Ne}$  at 80 MeV/nucleon from the K1200 cyclotron impinged on a 200 mg/cm<sup>2</sup>  $^9\text{Be}$  target. The fragmentation products were analyzed with the A1200 fragment separator [8], which provided  $3.5 \times 10^4$   $^{19}\text{Ne}$  ions per second at an energy of  $55.0 \pm 0.3$  MeV/nucleon. The beam was then delivered to a 518 mg/cm<sup>2</sup> Au target located at the focus of the NSCL position-sensitive NaI(Tl) array [9]. A fast-slow phoswich detector was placed downstream for positive identification of  $^{19}\text{Ne}$  ions deflected to  $\theta_{\text{lab}} < 5.0$  deg; this arrangement selects ions with a minimum impact parameter  $b_{\text{min}} = 13.0$  fm (17.5 fm) at the upstream (downstream) face of the target. The NaI(Tl) array detected deexcitation  $\gamma$  rays following inelastic scattering in coincidence with the identified  $^{19}\text{Ne}$  particles. The position information from the NaI array was used for relativistic Doppler correction of the measured photon energy.

A beam-frame photon spectrum, gated on  $^{19}\text{Ne}$  particles, prompts  $\gamma$ -ray times for background reduction, and photon multiplicity of one, are shown in Fig. 2. The deexcitation photon spectrum is complicated, owing to two factors. First, the decay of the individual states often involves non-negligible branches to other excited states, rather than directly to the ground state. Second, for the roughly 4 MeV photons emitted from high-lying states of interest, there is a high probability for escape of annihilation photons following pair production.

To determine excitation probabilities, GEANT simulations [10] were performed for the  $\gamma$  rays that were expected to be observed in the experiment. These simulations included intrinsic detector energy and position resolution and Doppler effects. The simulations predicted photopeak efficiencies of 8.10% and 4.28% for 0.898 and 1.836 MeV gamma rays from a fixed source. To test the simulations, the efficiency of the array was measured with a standard  $^{88}\text{Y}$  source, and the

\*Present address: GSI, Plankstrasse 1, D-64921 Darmstadt, Germany.

†Present address: Dept. of Physcs, Brookhaven National Laboratory, Upton, NY 11973.

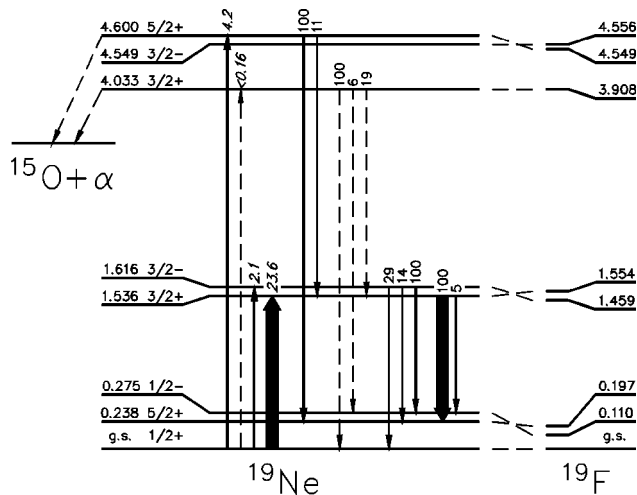


FIG. 1. Partial schematic energy level diagram for  $^{19}\text{Ne}$ . Solid vertical arrows indicate the Coulomb excitation (up) and subsequent  $\gamma$  decay (down) observed in the experiment. The numbers in italics are the excitation cross sections measured in this experiment in mb; all other numbers (excitation energies in MeV, spins and parities, and gamma relative branching ratios normalized to 100 for the strongest transition) are taken from the references. Dashed vertical arrows for the 4.033 MeV state indicate that these transitions were not positively identified in this experiment. Dashed oblique arrows indicate the  $\alpha$  decay branches to  $^{15}\text{O}$ ; the present work did not measure these. Also shown are selected levels in the mirror nucleus  $^{19}\text{F}$  with dashed lines identifying their analog states in  $^{19}\text{Ne}$ . See text for uncertainties and further details.

simulations agree with the measurement within the uncertainty of the  $^{88}\text{Y}$  source strength. The simulations also adequately described the observed spectral shape from the  $^{88}\text{Y}$  source [11]. We note that the simulations predict a photopeak efficiency of 2.10% for 4.362 MeV gamma rays.

The decay from a given state was modeled by taking the appropriate linear combinations of the simulated spectra using experimental branching ratios reported for  $^{19}\text{Ne}$  in Ref. [3]. These branching ratios themselves have measurement uncertainties, but the errors are correlated since the sum of the branching ratios must add up to 1. An error in the branching ratios, then, would simultaneously overpredict one branch and underpredict another, the net result being a second-order systematic effect which is much smaller than the statistical uncertainties in our measurement. The normalizations of these summed, simulated spectra for each state were then treated as free parameters in a MINUIT [12]  $\chi^2$  minimization to best fit the observed  $\gamma$ -ray spectrum. The simulated spectra for the decay of the 1.536, 1.616, 4.033, and 4.600 MeV states were used. All of these states could be excited by  $E1$ ,  $E2$ , or  $M1$  modes. The 4.549 MeV state could be populated by  $E1$  excitation, but it was not included in the fit because the data for the analog state in  $^{19}\text{F}$  indicated it would have a cross section much smaller than the experimental sensitivity. The fit included two exponential functions to model backgrounds. A broad Gaussian near 5.3 MeV was also required to fit the data; it may describe unresolved decay from  $E_x > 5$  MeV states for which little  $\gamma$  spectroscopic information is known [3].

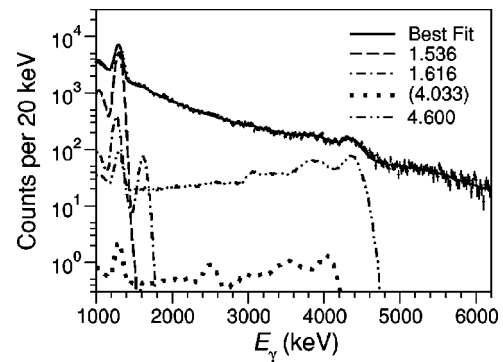


FIG. 2. Data points: energy spectrum of  $^{19}\text{Ne}$  deexcitation  $\gamma$  rays following intermediate-energy Coulomb excitation observed in the beam frame of reference. Solid curve: best fit to data. Broken curves: contributions to best fit from each of the four states included in the fit; for the 4.033 MeV state, the curve shows the  $2\sigma$  upper-limit yield. See text for details.

The best fit spectrum is shown in Fig. 2, and the results of the analysis are reported in Table I. All cross sections are corrected for photon angular acceptance bias by integrating the angular distributions calculated [13] for the dominant peak in the deexcitation spectrum. Based on the data for the 1.554 MeV mirror state in  $^{19}\text{F}$ , it was expected that the  $M1$  contribution to the excitation cross section for the  $^{19}\text{Ne}$  1.536 MeV state would be three orders of magnitude lower than that for  $E2$  excitation [1,3]. Mixing ratios for deexcitation  $\Delta J=1, \Delta\pi=0$  transitions are not known. For the 1.536 MeV state, this introduces a systematic  $\pm 13\%$  limit uncertainty. A further correction is needed for the  $\alpha$  decay branch of the 4.600 MeV state, for which  $\Gamma_\alpha/\Gamma_{\text{tot}}=0.25\pm 0.04$  [4]. Nucleon or light-ion decay modes are not energetically possible from this state and  $\beta$  decay would be negligible, so the  $\alpha/\gamma$  branching ratio can be determined from this value.

To extract the  $B(\sigma\lambda, 1/2_{\text{g.s.}}^+ \rightarrow J^\pi)$  reduced transition probability, given in Table I, the formalism of Winther and Alder [13] as implemented in the RELEX code [14] was used to calculate the expected cross section for unit  $B(\sigma\lambda)$  values, and this was then compared to the measured values. Midtarget kinematic parameters of  $\beta=0.307$ ,  $\theta_{\text{c.m.}} < 5.48$  deg, and  $b_{\text{min}}=15.3$  fm were used in these calculations. An uncertainty of 0.2 deg in the incidence angle of the  $^{19}\text{Ne}$  ions introduces a systematic effect due to uncertainty in  $b_{\text{min}}$ . There is also an uncertainty in the  $^{88}\text{Y}$  source strength. Together, these effects contribute a combined systematic uncertainty of 10%.

These transition rate measurements are compared to existing data for  $^{19}\text{Ne}$  and also to analog states in the mirror nucleus  $^{19}\text{F}$  in Table I. Data for  $^{19}\text{Ne}$  only exists for the  $^{19}\text{Ne}$  1.616 MeV state [3], and the lifetime measurements of this state following  $(\alpha, n)$  [15] and  $(p, n)$  [15,16] reactions are inconsistent with one another. These Doppler-shift attenuation measurement (DSAM) experiments following light-ion fusion-evaporation reactions would be unable to account for the effective lifetime of the gamma ray cascade feeding the states of interest, which would result in a larger apparent lifetime for the state. Hence, these transition rates should be regarded as lower limits.

TABLE I. Cross sections for excitation from the ground state and reduced transition probabilities measured in this experiment. Reduced transition probabilities are reported in units of  $10^{-4} e^2\text{fm}^2$  for  $E1$ ,  $e^2\text{fm}^4$  for  $E2$ , and  $\mu_N$  for  $M1$  transitions. The  $1\sigma$  errors are statistical and systematic, respectively. For the 4.033 MeV state, the reported  $B(\sigma\lambda)$  is the  $2\sigma$  upper limit. In the cross-section measurements, the dominant systematic error comes from ambiguous angular distributions from mixed  $M1/E2$  transitions; only in the case of the 1.536 MeV state is this not negligible compared to the statistical error. Also shown are values from previous measurements for two low-lying states and data from analog transitions in  $^{19}\text{F}$ , see text for details.

$^{19}\text{Ne}$					$^{19}\text{F}$				
$E_{\text{exc}}$ (MeV)	$J^\pi$	$\sigma\lambda$ exc.	$\sigma_{\text{exc}}$ (mb)	This work	$B(\sigma\lambda, \uparrow)$ Other meas.	Calc. <sup>a</sup>	$B(\sigma\lambda, \uparrow)$ Meas.	Calc. <sup>a</sup>	
1.536	$3/2^+$	$E2$	$23.6 \pm 0.3 \pm 3.1$	$79 \pm 1 \pm 18$		93.4	$50^b$	49.6	
1.616	$3/2^-$	$E1$	$2.1 \pm 0.3$	$18 \pm 3 \pm 2$	$4.2 \pm 0.8^{c,d}$		$9 \pm 2^c$		
4.033	$3/2^+$	$M1$	$-0.21 \pm 0.19$	$< 0.90^e$		0.045		0.044	
		$E2$	$-0.19 \pm 0.17$	$< 0.64^e$		0.80		1.28	
4.600	$5/2^+$	$E2$	$4.2 \pm 0.3$	$20 \pm 2 \pm 2$		24.4	$8^b$	7.0	
0.238	$5/2^+$	$E2$	f	f	$123 \pm 4^c$	132.8	$64.3 \pm 0.8^c$	68.9	
0.275	$1/2^-$	$E1$	f	f	$49 \pm 2^c$		$55.3 \pm 0.7^c$		

<sup>a</sup>Calculated as discussed in text.

<sup>b</sup>Derived from Ref. [1].

<sup>c</sup>From Ref. [3].

<sup>d</sup>Adopted value from DSAM experiments that are not in agreement; see discussion in text.

<sup>e</sup>These  $2\sigma$  limits assume unmixed transitions. For  $\delta = +0.14$ , the measured cross section places simultaneous limits of  $< 0.035 \mu_N$  on  $B(M1)$  and  $< 0.61 e^2\text{fm}^4$  on  $B(E2)$ .

<sup>f</sup>Not measurable in this experiment due to energy threshold effects.

Table I also includes full  $s$ - $d$  shell model calculations for  $^{19}\text{Ne}$  that are similar to those used in the analysis of  $^{19}\text{F}(e, e')$  data [1], which used effective  $M1$  and  $E2$  operators as discussed in Ref. [17]. The agreement with the data is quite good. In particular the calculated  $B(E2)$  values are larger in  $^{19}\text{Ne}$  than  $^{19}\text{F}$  for  $s$ - $d$  shell dominated transitions, which both agrees with experiment and with what one would expect since  $^{19}\text{Ne}$  has two valence protons whereas  $^{19}\text{F}$  has just one [18].

The  $2\sigma$  upper limit of the reduced transition probabilities for excitation of the 4.033 MeV  $3/2^+$  state from the ground state can be used to place an upper limit on the width for the  $\gamma$  branch to the ground state,  $\Gamma_{\gamma, \text{g.s.}}$ . Knowing the measured  $\gamma$  branching ratios to excited states [3], the total gamma width  $\Gamma_\gamma$  can be calculated.<sup>1</sup> Since the decay is dominantly electromagnetic,  $\Gamma \approx \Gamma_\gamma$ . The upper limit on the excitation cross section yields upper limits on  $\Gamma_\gamma$  of 430 meV (0.34 meV) for excitation and subsequent decay by pure  $M1$  ( $E2$ ) transitions. The mixing ratio  $\delta$ , where  $\delta^2 \propto (B(E2)/B(M1))E_\gamma^2$  is the ratio of  $E2$  and  $M1$  partial transition rates, is not known. However,  $M1$  dominance ( $\delta \sim 0$ ) is consistent with DSAM, where a reported  $2\sigma$  upper limit on lifetime corresponds to a  $\Gamma_\gamma > 6.6$  meV [19]. By

contrast,  $E2$  dominance ( $|\delta| \sim \infty$ ) is inconsistent with the DSAM data. Figure 3 demonstrates how the upper limit on  $\Gamma_\gamma$  for the  $^{19}\text{Ne}$  4.033 MeV  $3/2^+$  state varies depending on the mixing ratio  $\delta$ . The gamma width is compared to the DSAM measurement.  $E2$  excitation generally dominates intermediate-energy Coulomb excitation, so even a small  $E2$  admixture would decrease the total  $\Gamma_\gamma$  that would be consistent with the current measurement. For example, for

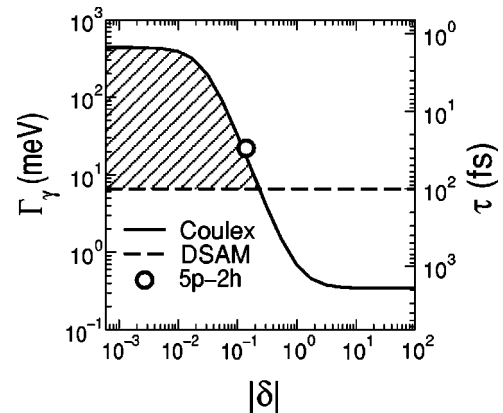


FIG. 3. Curves delimit  $2\sigma$  upper and lower limits on the total gamma width  $\Gamma_\gamma$  for the 4.033 MeV state from the present Coulomb excitation (Coulex) and lifetime (DSAM) data, respectively, as a function of the  $E2/M1$  mixing ratio for transitions to or from the ground state. Hatched area indicates overlapping region of  $2\sigma$  confidence from both measurements. The data point is the value expected for the matrix elements calculated as described in the text.

<sup>1</sup>The uncertainties in branching ratios are correlated and would introduce an additional  $\sim 10\%$  statistical uncertainty in the present measurement. Since the current data provide an upper limit, this effect is neglected in the discussion.

$|\delta|=0.03$ , the upper limit on  $\Gamma_\gamma$  is half that for  $\delta=0$ , and for  $|\delta|=0.23$  the upper limit is the same as the lower limit derived from the DSAM measurement [19]. From a different point of view, our results restrict this mixing ratio to  $|\delta|<0.23$  for the decay of the 4.033 MeV state to the ground state.

Before further discussion of our experimental results on the 4.033 MeV  $3/2^+$  state in  $^{19}\text{Ne}$ , it is worth noting that this state and its analog in  $^{19}\text{F}$  have long eluded a straightforward shell-model description. In the original analysis of Ref. [1], it was concluded that the second  $3/2^+$  state in  $^{19}\text{F}$  at 3.908 MeV did not have a three-particle ( $3p$ )  $s$ - $d$  shell configuration but was more likely a five-particle, two-hole ( $5p$ - $2h$ ) configuration with two nucleons excited from the  $p$  shell. In the present work, the energy of the  $5p$ - $2h$  configuration for the  $A=19$  mirror nuclei was calculated using the WBP Hamiltonian of Warburton and Brown [20]. The lowest eigenstate of the  $5p$ - $2h$  configuration indeed has  $J^\pi=3/2^+$  and an excitation energy of 4.50 MeV, which is in reasonable agreement with the experimental excitation energies of 4.033 and 3.908 MeV in  $^{19}\text{Ne}$  and  $^{19}\text{F}$ , respectively. However, the  $B(\sigma\lambda)$  values for pure  $3p$  to  $5p$ - $2h$  excitations vanish since they cannot be connected by a one-body electromagnetic operator. Mixing between the  $5p$ - $2h$  and  $3p$  configurations was calculated using the Kuo-Brown  $G$  matrix for the off-diagonal interaction as a perturbation; the reduced transition probabilities reported in Table I were extracted from the matrix elements calculated for the resulting mixed wave function. It should be noted that for these reduced transition probabilities, the  $M1$  Coulomb excitation probability in this experiment would be only 5% that of the  $E2$  excitation probability, but the corresponding partial gamma decay width would be 50 times greater. The  $5p$ - $2h$  calculations also yield matrix elements for decay of this  $3/2^+$  state to the first excited  $5/2^+$  and  $3/2^+$  states. These branches would be 20% and 55% as intense as the decay directly to the ground state in  $^{19}\text{Ne}$ , and 30% and 63% in  $^{19}\text{F}$ . These compare well to the measured branching ratios [3], suggesting that the present model is reasonable and can be used to describe the second  $3/2^+$  state in the  $A=19$  mirror nuclei.

The results of the  $5p$ - $2h$  calculations may now be compared to our experimental results on the  $^{19}\text{Ne}$   $3/2^+$  state at 4.033 MeV. Taking the calculated matrix elements for the  $5p$ - $2h$  state and the observed excitation energy and  $\gamma$  branching ratios,  $\Gamma_{\gamma,5p2h}=22$  meV and  $\delta_{5p2h}=+0.14$ . This point is plotted on Fig. 3. Furthermore, one may use the calculated value of the mixing ratio  $\delta$  along with the measured Coulex cross sections to better constrain the upper limit on  $\Gamma_\gamma$ . As indicated in Table I, for the value of  $\delta_{5p2h}$  from the calculations, the present experiment would limit  $B(M1)<0.035 \mu_N$  and  $B(E2)<0.61 e^2\text{fm}^4$ , with a resulting limit of  $\Gamma_\gamma<17$  meV. For the decay of the corresponding 3.908 MeV state in  $^{19}\text{F}$ , the  $5p$ - $2h$  calculations yield  $\Gamma_\gamma=28$  meV and  $\delta=-0.18$ . The gamma width of this state in  $^{19}\text{F}$  has been reported as  $\Gamma_\gamma=75_{-25}^{+100}$  meV [21], while angular distribution measurements [22] are stated to be consistent with  $\delta\sim 0$ , although this depends on an assumption that the feeding transition is itself a pure dipole transition.

While the current measurement on its own only provides an upper limit on  $\Gamma_\gamma$ , it can be considered with other data to provide an estimate of  $\Gamma_\gamma$ . The present upper limit on the gamma width,  $\Gamma_\gamma\pm\sigma_\Gamma$ , and the DSAM measurement of the lifetime,  $\tau\pm\sigma_\tau$ , are two independent data points. If the width of the state is treated as a free parameter  $\Gamma_{\gamma p}$ , then there is an associated goodness-of-fit function  $\chi^2(\Gamma_p)=[(\Gamma_{\gamma p}-\Gamma_\gamma)/\sigma_\Gamma]^2+[(\hbar/\Gamma_{\gamma p}-\tau)/\sigma_\tau]^2$  indicating how well that parameter fits the Coulomb excitation and DSAM data. Minimizing this function determines the best estimate of the width, and finding the points at the minimum plus one determines the  $1\sigma$  uncertainties. The mixing ratio is unknown, and the absolute lowest  $\chi^2$  occurs for  $\delta=0$ , that is, assuming pure  $M1$  excitation and decay. This provides an estimate of the  $\Gamma_\gamma$  width of the  $^{19}\text{Ne}$  4.033 MeV state of  $45_{-33}^{+200}$  meV. For the purposes of stellar model calculations or for planning future experiments, it would be appropriate to constrain the experimental results further by adopting the mixing ratio  $\delta=+0.14$  calculated in the  $5p$ - $2h$  shell model. This lowers the  $\Gamma_\gamma$  upper limit from the Coulex data, yielding a better estimate of  $\Gamma_\gamma=12_{-5}^{+9}$  meV. Although this is the best estimate based on all of the available data, it must be noted that it does not take into account the uncertainty in the calculated mixing ratio  $\delta$ , which is itself difficult to estimate. In this particular experiment, the estimated width varies as  $\delta^{-1.8}$  in the vicinity of the calculation, so that an uncertainty of 5% in the mixing ratio calculation would increase the upper limit on the estimate by 2 meV.

Measurements of the  $^{15}\text{O}(\alpha,\gamma)$  reaction by accelerating radioactive  $^{15}\text{O}$  ions on a gaseous helium target are being planned for various radioactive beam facilities [23]. However, these experiments will be extremely difficult, requiring high-intensity beams and extremely clean analysis systems. They are not assured of success. For this reason, there are attempts to measure the branching ratio  $\Gamma_\alpha/\Gamma_\gamma$  for the decay of the 4.033 MeV state following its formation in a reaction [24]. These measurements are also difficult, and will still require the previously unknown value of  $\Gamma_\gamma$  to obtain  $\Gamma_\alpha$ . The present data provide an estimate of  $\Gamma_\gamma$  that can be used along with branching ratio data to calculate the astrophysical reaction rate. In addition, the data provide guidance for future high-resolution  $\gamma$  spectroscopy studies. A measurement of the mixing ratio for the  $^{19}\text{Ne}$  4.033 MeV  $\gamma$  ray could further constrain the values of  $\Gamma_\gamma$  that are consistent with the Coulomb excitation and lifetime data. Also, the current measurement establishes a lower limit of 1.8 fs for the 4.033 MeV state that can be used to evaluate the feasibility of future DSAM experiments.

In conclusion, an intermediate-energy Coulomb excitation measurement of the radioactive  $^{19}\text{Ne}$  nucleus has been performed. Reduced transition probabilities for excitations to selected states are reported and found to be in reasonable agreement with expectations based on isospin symmetry and  $s$ - $d$  shell model calculations. The upper limit on the excitation cross section of the 4.033 MeV  $3/2^+$  state yields an upper limit of 430 meV if the transition is pure magnetic



dipole. Shell-model calculations with  $5p$ - $2h$  configurations yield  $\Gamma_{\gamma,5p2h}=22$  meV and  $\delta_{5p2h}=+0.14$ . Using the experimental cross sections from the current experiment, the calculated mixing ratio, and the limits from a prior DSAM experiment, the estimate of the total gamma width is  $\Gamma_{\gamma}=12_{-5}^{+9}$  meV.

This work was supported by the National Science Foundation under Contract Nos. PHY-9528844, PHY-9875122, and PHY-9605207. G.H. also acknowledges support from the University of Kansas General Research Fund and the U.S. Department of Energy, Contract No. DE-FG03-96ER40981.

- 
- [1] B.A. Brown, B.H. Wildenthal, C.F. Williamson, F.N. Rad, S. Kowalski, Hall Crannel, and J.T. O'Brien, *Phys. Rev. C* **32**, 1127 (1985).
- [2] R.K. Wallace and S.E. Woosley, *Astrophys. J., Suppl. Ser.* **28**, 247 (1981).
- [3] D.R. Tilley, H.R. Weller, C.M. Cheeves, and R.M. Chasteler, *Nucl. Phys.* **A595**, 1 (1995).
- [4] P.V. Magnus, M.S. Smith, A.J. Howard, P.D. Parker, and A.E. Champagne, *Nucl. Phys.* **A506**, 332 (1990).
- [5] Z.Q. Mao, H.T. Fortune, and A.G. Lacaze, *Phys. Rev. C* **53**, 1197 (1996).
- [6] F. de Oliveira *et al.*, *Phys. Rev. C* **55**, 3149 (1997).
- [7] T. Glasmacher, *Annu. Rev. Nucl. Part. Sci.* **48**, 1 (1998); H. Scheit *et al.*, *Phys. Rev. Lett.* **77**, 3967 (1996); M.J. Chromik, B.A. Brown, M. Fauerbach, T. Glasmacher, R.W. Ibbotson, H. Scheit, M. Thoennessen, and P.G. Thirolf, *Phys. Rev. C* **55**, 1676 (1997); R.W. Ibbotson, T. Glasmacher, P.F. Mantica, and H. Scheit, *ibid.* **59**, 642 (1999).
- [8] B.M. Sherill *et al.*, *Nucl. Instrum. Methods Phys. Res. B* **56**, 1106 (1991).
- [9] H. Scheit *et al.*, *Nucl. Instrum. Methods Phys. Res. A* **422**, 124 (1999).
- [10] S. Giani *et al.*, GEANT v.3.21, CERN Long Writeup W5013, 1994 (unpublished).
- [11] G. Hackman *et al.*, NSCL Annual Report 1999 (unpublished).
- [12] F. James, MINUIT v.94.1, CERN Long Writeup D506, 1994 (unpublished).
- [13] A. Winther and K. Alder, *Nucl. Phys.* **A319**, 518 (1979).
- [14] C.A. Bertulani, *Comput. Phys. Commun.* **116**, 345 (1999).
- [15] R.D. Gill, K. Bharuth-Ram, K.P. Jackson, R.A.I. Bell, B.C. Robertson, J. L'Ecuyer, N.G. Chapman, and H.J. Rose, *Nucl. Phys.* **A152**, 369 (1970).
- [16] C. Lebrun, F. Guilbault, P. Avignon, and Y. Deschamps, *Phys. Rev. C* **15**, 1174 (1977).
- [17] B.A. Brown and B.H. Wildenthal, *Annu. Rev. Nucl. Part. Sci.* **38**, 29 (1988); M.C. Etchegoyen, A. Etchegoyen, B.H. Wildenthal, B.A. Brown, and J. Keinonen, *Phys. Rev. C* **38**, 1382 (1988).
- [18] E.K. Warburton and J. Weneser, in *Isospin in Nuclear Physics*, edited by D.H. Wilkinson (North-Holland, Amsterdam, 1969), p. 173.
- [19] J.M. Davidson and M.L. Roush, *Nucl. Phys.* **A213**, 332 (1973); this reference reports  $1\sigma$  limits.
- [20] E.K. Warburton and B.A. Brown, *Phys. Rev. C* **46**, 923 (1992).
- [21] W.R. Dixon, T.J.M. Symons, A.A. Pilt, K.W. Allen, C.H. Zimmerman, F. Watt, and S.P. Dolan, *Phys. Lett.* **62A**, 479 (1977).
- [22] J.P. Allen, A.J. Howard, D.A. Bromley, and J.W. Olness, *Phys. Rev. B* **140**, B1245 (1965).
- [23] For example, J.M. D'Auria, in *Proceedings of the International Workshop on JHF Science*, edited by J. Chiba *et al.* (KEK 98-5) (Tsukuba, 1998) Vol. I, p. 118.
- [24] A.M. Laird *et al.*, in *Experimental Nuclear Physics in Europe, ENPE 99: Facing the Next Millennium*, Sevilla, Spain, 1999, edited by Berta Rubio, Manolo Lozano, and William Gelletly, AIP Conf. Proc. No. 495 (AIP, New York, 1999), p. 2367; E. Rehm (private communication); M. Wiescher (private communication).